FISEVIER

Contents lists available at ScienceDirect

Microvascular Research

journal homepage: www.elsevier.com/locate/ymvre



Regular Article

Calpain- and talin-dependent control of microvascular pericyte contractility and cellular stiffness

Maciej Kotecki ^a, Adam S. Zeiger ^b, Krystyn J. Van Vliet ^{b,c,*}, Ira M. Herman ^{a,*}

- a Department of Physiology, and The Center for Innovations in Wound Healing Research, Tufts University School of Medicine, 150 Harrison Avenue, Boston, MA 02111, USA
- ^b Department of Materials Science and Engineering, Massachusetts Institute of Technology, 77 Massachusetts Avenue, Cambridge, MA 02139, USA
- ^c Department of Biological Engineering, Massachusetts Institute of Technology, 77 Massachusetts Avenue, Cambridge, MA 02139, USA

ARTICLE INFO

Article history: Accepted 30 July 2010 Available online 12 August 2010

Keywords:
AFM
Actin
Angiogenesis
Capillary
Cytoskeleton
Cell shape
Extracellular matrix
Diabetic retinopathy
Focal adhesions
Macular degeneration
Mechanotransduction

ABSTRACT

Pericytes surround capillary endothelial cells and exert contractile forces modulating microvascular tone and endothelial growth. We previously described pericyte contractile phenotype to be Rho GTPase- and α smooth muscle actin (αSMA)-dependent. However, mechanisms mediating adhesion-dependent shape changes and contractile force transduction remain largely equivocal. We now report that the neutral cysteine protease, calpain, modulates pericyte contractility and cellular stiffness via talin, an integrin-binding and Factin associating protein. Digital imaging and quantitative analyses of living cells reveal significant perturbations in contractile force transduction detected via deformation of silicone substrata, as well as perturbations of mechanical stiffness in cellular contractile subdomains quantified via atomic force microscope (AFM)-enabled nanoindentation. Pericytes overexpressing GFP-tagged talin show significantly enhanced contractility (~two-fold), which is mitigated when either the calpain-cleavage resistant mutant talin L432G or vinculin are expressed. Moreover, the cell-penetrating, calpain-specific inhibitor termed CALPASTAT reverses talin-enhanced, but not Rho GTP-dependent, contractility. Interestingly, our analysis revealed that CALPASTAT, but not its inactive mutant, alters contractile cell-driven substrata deformations while increasing mechanical stiffness of subcellular contractile regions of these pericytes. Altogether, our results reveal that calpain-dependent cleavage of talin modulates cell contractile dynamics, which in pericytes may prove instrumental in controlling normal capillary function or microvascular pathophysiology. © 2010 Elsevier Inc. All rights reserved.

Introduction

Regulation of microvascular remodeling during physiologic and pathologic angiogenesis involves multiple, dynamic interactions between endothelial cells (EC) and pericytes (Jain, 2003; Folkman, 1971; Kutcher and Herman, 2009). Pericytes surround the capillary endothelium, communicating directly through the basement membrane via gap junctions or soluble factors: these interactions modulate microvascular stability, angiogenesis, capillary contractility and blood flow (Kutcher and Herman, 2009; Darland and D'Amore, 1999; Rucker et al., 2000). Indeed, pericyte–EC associations have been demonstrated to regulate vascular maturation (Darland and D'Amore, 2001a), and it has been conclusively established that soluble mediators and pericyte contacts control EC growth and survival via TGF-beta and VEGF (Darland and D'Amore, 2001b; Darland et al., 2003; Shih et al., 2003; Sieczkiewicz and Herman, 2003; Papetti et al., 2003).

Reciprocally, ECs are postulated to recruit and maintain differentiated pericytes in the microvascular niche via growth factors including FGF-2 (Healy and Herman, 1992) and PDGF (Bjarnegard et al., 2004; Wilkinson-Berka et al., 2004). Such pericyte–EC interactions modulate EC proliferation (Orlidge and D'Amore, 1987) and migration (Sato and Rifkin, 1989), prevent microvascular regression (Benjamin et al., 1998), and can stabilize nascent microvessels during development (von Tell et al., 2006). Finally, we have recently demonstrated that pericyte contraction is sufficient to modulate the mechanical niche of adjacent EC, either via direct contractile strain or indirect modulation of the mechanical stiffness of strained basement membrane (Lee et al., 2010). Thus, it is becoming increasingly apparent that pericytes play key regulatory roles in modulating microvascular remodeling, capillary contractility and blood flow.

Pericyte control of microvascular remodeling and capillary tonus has been implicated as dependent on Rho GTP, Rho kinase, and isoactin (Kutcher and Herman, 2009; Kolyada et al., 2003; Kutcher et al., 2007). Indeed, previous studies have revealed that signaling through pericyte Rho GTP enhances pericyte contractility specifically through the α -smooth muscle actin (α SMA) cytoskeletal network. Furthermore, pericyte control of EC proliferation is similarly sensitive to pericyte-dependent contractility, since modulating pericyte Rho

^{*} Corresponding authors. K.J. Van Vilet is to be contacted at Department of Materials Science and Engineering, Massachusetts Institute of Technology, 77 Massachusetts Avenue, Cambridge, MA 02139, USA.

E-mail addresses: krystyn@mit.edu (K.J. Van Vliet), ira.herman@tufts.edu (L.M. Herman).

GTP reversibly regulates endothelial growth regardless of whether pericytes and EC are in direct cell contact (Kutcher et al., 2007). In this way, pericyte mechanotransduction may prove instrumental in modulating EC growth during pathologic angiogenesis that would not depend on "pericyte dropout" or death as the initiating signal/event (Kutcher and Herman, 2009; Kutcher et al., 2007).

If mechanical force transduction plays an instrumental role in regulating endothelial dynamics during physiologic or pathologic angiogenesis, then one might posit that the key interface of interest is the cell membrane, which links the cytoskeleton to the extracellular matrix or adjacent cells through specific adhesive ligand-receptor complexes. Indeed, macromolecular focal adhesion complexes or FAs coordinate such dynamic interactions and participate in force transduction. Transmembrane integrins are key FA components that act as adhesion receptors via binding to extracellular matrix (ECM) ligands (Hynes, 2002; Berrier and Yamada, 2007). These integrins cluster in a calpain-dependent manner (Bialkowska et al., 2000); the active remodeling of these FA-cytoskeletal protein assemblies occurs by recruiting cytoskeletal actin adaptors and regulators via β-integrin cytoplasmic tails. Key adaptor proteins include vinculin, α -actinin, paxillin, zyxin and talin (Zamir and Geiger, 2001; Zaidel-Bar et al., 2007). Among these FA components, talin 1 not only binds and activates integrins (Banno and Ginsberg, 2008; Wegener et al., 2007; Moes et al., 2007), but also binds to F-actin (Gingras et al., 2008), providing a direct link between the ECM and cytoskeleton, Talin 1 increasingly binds to vinculin under applied mechanical strain, and signals cytoskeletal remodeling (Izard and Vonrhein, 2004; del Rio et al., 2009). Consequently, talin 1 is considered a key player in FA mechanosensory function, coordinating cell adhesion and supporting mechanotransduction while reinforcing integrin-cytoskeletal interactions (del Rio et al., 2009; Arnaout et al., 2007; Roberts and Critchley, 2009; Roca-Cusachs et al., 2009).

Previous studies have suggested that FA remodeling, including talin's role in coordinating membrane-cytoskeleton interactions, is regulated by the calcium-dependent protease, calpain (Franco et al., 2004; Franco and Huttenlocher, 2005). This family of proteases is broadly implicated in cellular processes such as proliferation, differentiation, apoptosis, adhesion, spreading, migration and angiogenesis (Croall and Ersfeld, 2007; Goll et al., 2003; Ma et al., 2009), as well as in pathologies such as retinal degeneration (Paquet-Durand et al., 2007; Azuma and Shearer, 2008) and cancer cell invasion (Cortesio et al., 2008). Activity of two major isoforms, calpain 1 and calpain 2, is tightly regulated in a spatially and temporally specific fashion by phosphorylation, calcium binding-requirement, and by a specific cellular inhibitor, calpastatin (Franco and Huttenlocher, 2005; Hanna et al., 2008). Indeed, others have demonstrated the key roles that calpains play in modulating cytoskeletal dynamics during cell spreading and migration (Shuster and Herman, 1995; Huttenlocher et al., 1997; Croce et al., 1999; Potter et al., 1998). In addition, calpain is required for the formation of nascent integrin clusters, which evolve into active Rac-containing focal complexes and into active RhoAcontaining FAs (Kulkarni et al., 1999). More recently, it has been shown that the FA dynamics are regulated by calpain cleavage of talin, since the expression of the calpain-resistant talin mutant L432G perturbs FA protein turnover (Franco et al., 2004).

Considering the pivotal role of pericytes in modulating microvascular morphogenesis *in vivo*, the connection between pericyte contraction and EC proliferation *in vitro*, and finally the regulation of FA dynamics by calpain, we have become interested in exploring the mechanisms that calpain may play in pericyte contractile force and, in turn, capillary contractility. Here, we report a series of experiments designed to test directly whether talin and calpain have the ability to regulate pericyte contractility. Using purified populations of bovine retinal pericytes and a deformable silicone substratum contractility assay, we compared the contractile phenotype of pericytes overexpressing GFP-tagged talin with those bearing a talin L432G mutant

that is resistant to calpain cleavage. In related experiments, we quantified the influence of overexpressed vinculin and constitutively activated RhoA Q63L on pericyte contractility. Finally, to explore the molecular mechanisms controlling pericyte contractility in response to talin and Rho GTP-dependent signaling, we conducted atomic force microscopy (AFM)-enabled nanoindentation to quantify the subcellular stiffness of pericytes in situ, in the presence of a cell-penetrating calpain-specific inhibitor developed in our laboratory, termed CALPASTAT, and its inactive point mutant (Croce et al., 1999). Together, these experiments demonstrate that calpain-mediated signaling, in concert with talin, is a critical component of interactions at the pericyte cytoskeleton-membrane interface that regulate cell contractility and local cell stiffness. In turn, these observations may lend important insights into the manner in which chemomechanical force transduction and cytoskeletal-membrane signaling networks coordinate microvascular phenomena during development or disease.

Materials and methods

Cell culture

Primary cultures of bovine retinal pericytes (BRP) were isolated and characterized as described previously (Herman and D'Amore, 1985). Vascular smooth muscle actin (SMA)-, NG2 proteoglycan- and 3G5-positive and CD-31- and di-I-acyl-LDL-negative pericyte cultures were grown in Dulbecco's modified Eagle's medium (DMEM) supplemented with penicillin, streptomycin, Fungizone (all from Invitrogen, Carlsbad, CA) and 10% calf serum (CS, from Atlanta Biologicals, Lawrenceville, GA), and used for experiments between passages 2 and 4. Pericytes were grown in tissue culture plasticware (Corning, Inc., Corning, NY): T175 flasks (for expansion prior to experiments) and vessels of 24-well plate or 8-chamber slide format (for experiments proper), in a total volume of 1 ml per well or 0.5 ml per chamber, while incubated at 37 °C in 5% CO₂ atmosphere.

Plasmids

The following plasmids were used: pEGFP-C1 empty vector (Clontech Inc., USA) expressing enhanced green fluorescent protein, EGFP-C1 fusion with mouse talin 1 and talin 1 mutant L432G (courtesy of Dr. A. Huttenlocher, University of Wisconsin-Madison), EGFP-C1 fusion with vinculin (courtesy of Dr. Susan Craig, Johns Hopkins University), pExv and pExv/RhoA (Q63L) expressing dominant active form of RhoA (RhoDA) (courtesy of Dr. Deniz Toksoz, Tufts University). Plasmid DNAs were prepared with endotoxin-free maxi kits (Qiagen).

Electroporation

One day before electroporation, pericytes were seeded at a density of $0.5-0.7 \times 10^6$ pericytes per T175, to obtain ca. 60–70% confluency on the next day. The electroporation mixture was prepared in a 1.5 ml tube by including (per sample) 18 µl of supplement and 82 µl of solution (both from Basic Nucleofactor Kit for Primary Endothelial Cells, Lonza, Cat. No. VpI-1001), and 15 µg of plasmids expressing EGFP fusion constructs or 12 µg of RhoA Q63L plasmid mixed with 3 μg of pEGFP-C1 plasmid (4:1 ratio). This mixture (110–120 μl) was added to $0.5-1\times10^6$ pericytes, which were freshly harvested (trypsinized, counted in hemacytometer, washed and spun in 10 ml of growing medium in 15 ml conical tubes, in a bench top Sorvall RT6000B centrifuge at 700 rpm, 10 min at room temperature). Cells gently re-suspended in electroporation mixture were transferred to individual 4 mm electroporation cuvettes and electroporated using Harvard Apparatus BTX electroporator set for 2 pulses of 5 ms each at 200 V, with an interval of 1 s. Five minutes after electroporation, 0.5 ml of growing medium was added to each cuvette with electroporated cells, and the whole volume was transferred to a 15 ml tube, raised with growing medium to an appropriate volume and dispensed into duplicate experimental culture vessels. Using these constructs, electroporation-optimized transfection efficiently yields up to 45% GFP-positive cellular transfectants as ascertained by flow cytometry vs. 2–10% transfectants typically achieved using standard cationic lipid-based transfection reagents. Only electroporation was used as a method to obtain data from experiments involving overexpression of proteins in the bovine primary pericytes in this study.

Analysis of pericyte contractile phenotype

Preparation of deformable silicone substrates

Deformable silicone substrata for analysis of pericyte contractility in cultures were prepared as described previously (Harris et al., 1980; Kutcher et al., 2007) with the following modifications. Eight microliters of silicone (dimethylpolysiloxane, Sigma cat. # DMPS12M-100G) was pipetted with a positive displacement pipette to spread for 1 h at 42 °C onto round 12 mm glass coverslips or chambers of 8-chamber glass culture slide, from which plastic dividers were removed. Silicone on glass coverslips or slides was thermally crosslinked by passing through a Bunsen burner flame. A glow plasma discharge apparatus (Aebi and Pollard, 1987) was used to generate a plasma discharge onto silicone-coated coverslips or chamber slides (1 min vacuum pump, followed by 1 min discharge). After re-assembling plastic dividers onto glass culture slides or placing coverslips into wells of a 24-well plate, the charged silicone surface was coated with 100 μl of 0.1 mg/ml Type I collagen (BD Biosciences) in PBS and UV irradiated for 3 min in a sterile hood, enabling subsequent cell attachment in the transiently hydrophilic environment. Approximately $2-4\times10^3$ cells in 0.5 ml of growing medium were seeded onto prepared silicone-coated coverslips or chamber slides and cultured for 24 h prior to experiments unless otherwise noted.

Quantification of contractile force production in pericytes

On the next day after seeding, silicone-attached pericytes within 8-chamber culture slides or 24-well plates were examined via optical microscopy. Samples were mounted onto the motorized Ludl stage of a Zeiss Axiovert 200M computer-assisted light microscope imaging workstation within a 37 °C stabilized, temperature-controlled environment, to enable live cell viewing for protracted periods of time. Corresponding phase contrast and fluorescent microscopic images were acquired and overlaid for morphometric analysis using Metamorph software (Universal Imaging Corp.). Pericyte deformation of silicone substratum was scored as a manifestation of the cell contractile phenotype. In order to quantify the contractile phenotype of the cells, we defined an original parameter, designated as cell contractility index (CCI), which describes the extent of contraction in terms of number and length of substrata wrinkles per cell. We define CCI as the normalized wrinkle index (WI_{experimental sample}/WI_{control}). We define this wrinkle index as a weighted average of long and short wrinkles per actively contracting cell: WI = $(W_L + 0.5 \times W_S)/n$, where W_L is the number of long wrinkles (spanning more than half of the cell width at the wrinkle location), W_S is the number of short wrinkles (spanning less than half the cell width), and n is the number of actively contracting cells analyzed in a given culture condition. Actively contracting cells were those cells that visibly wrinkled the silicone substrata at the instance of WI measurement (24 h unless otherwise stated). Note that short wrinkles were generally observed less frequently than long ones, and we corrected for the apparently lower magnitude of contractile force at short wrinkles by halving this contribution to WI. In experiments with transfected EGFP plasmids, CCI was analyzed in contracting cells expressing EGFP fusion proteins. The normalized wrinkle index, CCI, was scored from at least 25 contracting cells in each experimental condition, and CCI of the control sample was set equal to 1 in all stated results. Data from at least three independent experiments were graphed and analyzed for p value of statistical significance (t-test of two-samples assuming unequal variances). In the text and the figures, CCI values are presented as the average \pm standard error of measurement. The difference between two CCI data sets was considered statistically significant when p<0.05.

Calpain inhibitors

Calpastat (abbreviated CALPST) is a synthetic 40 amino acid peptide previously developed in our laboratories and described to be a specific, cell-penetrating inhibitor of calpain activity and calpain-dependent *in vivo* cleavage of target proteins, including talin (Croce et al., 1999; Potter et al., 2003). This peptide was synthesized and purified at Tufts University Core Facility, reconstituted to a 25 mM stock in 0.1 M HEPES, pH 7.4, and used at final concentrations of 5, 25 or 100 µM to treat pericyte cultures. The alanine-substituted mutant of CALPST, termed CALPST-ala, was also described above (Croce et al., 1999) as an inactive control; this mutant was synthesized, prepared and used in the same fashion as CALPST.

Measurement of local elastic moduli with atomic force microscopy

An atomic force microscope (AFM; PicoPlus, Agilent Technology) was incorporated within an inverted optical microscope (IX81, Olympus) to enable facile positioning of AFM cantilevered probes above pericyte apical surfaces (see Fig. 4). All mechanical characterization experiments were conducted on living pericytes in full media at room temperature. Calibration of AFM cantilevers of nominal spring constant k = 0.01 nN/nm and nominal probe radius R = 25 nm(MLCT-AUHW, Veeco) was conducted as described previously (Thompson et al., 2006). Briefly, inverse optical lever sensitivity [nm/V] (InvOLS) was measured from deflection-displacement curves recorded on rigid glass substrates. Spring constants [nN/nm] of AFM cantilevers were measured via thermal activation recording of deflection, and the Fast Fourier Transform of cantilever free-end amplitude as a function of oscillation frequency was fitted as a harmonic oscillator to obtain this value. For each measurement of effective elastic moduli at any given location on any given cell, at least 30 replicate indentations were acquired to maximum depths of 10 nm. At least five cells were analyzed for each condition, and multiple indentation locations (i.e., wrinkle positions) were associated with each cell, as indicated in figure captions. Acquired probe deflectiondisplacement responses were converted offline (Scanning Probe Imaging Processor, Image Metrology), using measured spring constants and InvOLS, to force-depth responses. Effective elastic moduli $E_{\rm eff}$ were calculated by applying a modified Hertzian model of spherical contact to the loading segment of the force-depth response, as detailed elsewhere (Lee et al., 2010; Thompson et al., 2005) with the scientific computing software Igor Pro (Wavemetrics). These $E_{\rm eff}$ values represent the local stiffnesses of the subcellular domains probed in each experiment under contact loading, and are not intended to indicate the elastic properties of the entire cell or the Young's elastic modulus under uniaxial loading. In Fig. 4, local cell stiffness values are normalized by $E_{\rm eff}$ measured in untreated cells at subcellular domains located just above positions of substrata wrinkles. We have shown through previous AFM and fluorescence imaging that these locations correspond to regions of cell contraction that comprise F-actin stress fibers (Lee et al., 2010). Hereafter, subcellular domains corresponding to locations above wrinkles are denoted as "wrinkled domain" and subcellular domains corresponding to locations far from substrata wrinkles as "unwrinkled domain". This terminology is intended to contrast the local cell stiffness at sites of sustained contraction to that at sites remote from such visible contraction, within the same cell. As in

the wrinkling index observations described above, only actively contracting cells (i.e., those producing substrata wrinkles) were analyzed.

Before elastic moduli measurement via AFM-enabled nanoindentation, *x*- and *y*-axes hystereses of the closed loop piezoscanner were calibrated to improve the positioning of AFM cantilevered probes on pericyte membranes and silicone substrata. The force that AFM cantilevers exerted on pericyte membranes during contact mode imaging did not exceed 500 pN, which was chosen to minimize the effect of mechanical contact between pericytes and AFM cantilevers during imaging that preceded mechanical characterization of subcellular domains.

Computed elastic moduli $E_{\rm eff}$ are reported as average \pm standard error of measurement. All statistical analyses were conducted with one-way ANOVA (Tukey analysis), with statistical significance in stiffness differences considered at p < 0.05.

Results

Talin enhances pericyte contractility in calpain-dependent fashion

Previous work demonstrated a role for Rho GTP-dependent signaling in regulating pericyte and isoactin-dependent contraction in vitro (Kolyada et al., 2003; Kutcher et al., 2007). In an effort to identify the upstream and downstream modulators that control contractile phenotype, we now focus on that the roles of key focal adhesion and cytoskeletal associated proteins in orchestrating pericyte contractile force exertion against adherent substrata. Since talin is a key FA component that binds integrin and F-actin, and because these integrin-cytoskeletal associations have been demonstrated to be calpain-sensitive (Franco et al., 2004), we were eager to learn whether overexpressing talin and vinculin or perturbing calpain-mediated signaling might influence cellular contractility or stiffness. To directly assess the FA-mediated and calpain-dependent regulation of force production in retinal pericytes, we utilized a single cell-based contractility assay of cells grown to subconfluence on a thin sheet of deformable silicone substrata (see Materials and Methods). In particular, we analyzed contractility of retinal pericytes (RP) overexpressing control enhanced green fluorescent protein (EGFP), EGFPtalin, an EGFP-calpain-resistant mutant talin L432G, or EGFPvinculin. Similarly, we took advantage of a Rho GTP expression plasmid, namely a dominant active mutant RhoA Q63L, co-expressed with control EGFP constructs.

In order to quantify contractile force transduction exerted by individual pericytes, we analyzed cell-derived deformation of the elastic substratum directly underlying each contractile cell. Real-time, digital imaging affords the opportunity to assess cellular dynamics and contractility. Reviewing static images derived from these living cell studies enables a quantitative analysis of the Cell Contractility Index (CCI; see Materials and Methods). The CCI proposed here takes into account not only the number but also the extent of substratum deformation events (i.e., local wrinkling of the substratum). Generally, we observed no preferential distribution of substrata wrinkles in relation to distal tips of extending filopodia, lamellar membrane ruffles or pseudopodial extensions engaging isotonically contracting cytoskeletal domains. With processes that are actively extending forward we observe that substrate deformation is confined to the well anchored regions, which are closer to the cell body (focal adhesion-rich domains). The accuracy of quantifying contractility in terms of CCI can further be validated by positive control experiments, wherein overexpression of dominant active RhoA Q63L demonstrated enhanced retinal pericyte contractility (CCI = 1.44 ± 0.18 , p < 0.05, Fig. 1B) as compared to the pericytes expressing vector alone. These findings are consistent with previous work describing RhoA Q63L expression in pericytes (Kutcher et al., 2007). Using CCI analysis of pericytes expressing constructs of interest and plated upon deformable silicone substrates, we observe that pEGFP-talin overexpression significantly enhances pericytes contractility $(1.89\pm0.12,\ p<4\times10^{-9})$, when compared to EGFP-expressing control cells (Fig. 1B). The point mutant of talin L432G, which has been demonstrated previously to be resistant to calpain cleavage (Franco et al., 2004), exhibits no statistically significant change in CCI $(1.11\pm0.12,\ p=0.44)$ as compared to the control EGFP-expressing cells. Interestingly, we observed that overexpression of EGFP-vinculin, another protein component of focal adhesions and a target of calpain cleavage, does not cause any statistically significant change in pericyte contractility $(0.95\pm0.11,\ p=0.77,\ \text{Fig. 1B})$ as compared to the control cells. These results indicate the important role of talin, but not vinculin, in modulating calpain-dependent cellular force transduction.

Calpain controls talin-enhanced, but not active RhoA-dependent pericyte contractility

Given that wild-type talin enhances pericyte contractility, and the calpain-resistant talin mutant L432G does not, we hypothesized that the CCI-enhancing effect of talin's overexpression would be reversible by calpain-specific pharmacologic inhibitors. To test this hypothesis, we took advantage of our previously described calpastatin-derived and cell-penetrating synthetic peptide, CALPASTAT (hereafter abbreviated as CALPST), which was reported to penetrate cells in vivo and specifically inhibit calpain activity (Croce et al., 1999). As a control, we used a cell-penetrating alanine-substituted mutant of CALPST (CALPST-ala), which was also previously described to be inactive in inhibiting calpain activity and unable to prevent cleavage of calpain targets such as talin (Croce et al., 1999). These calpain-specific inhibitors were added to living cell cultures following RP plating onto deformable substrata. As can be observed from Fig. 2, CALPST concentrations of 5 and 25 µM do not have a statistically significant effect on CCI at 24, 48 or 96 h. However, 100 µM CALPST inhibits CCI by 48 h, down to 0.65 ± 0.06 of the untreated control (p < 0.0004); note that 100 μ M CALPST-ala control does not influence CCI (p<0.01). By 96 h of 100 μM CALPST treatment, CCI inhibition is ~50% of control values $(p<2\times10^{-7})$, with 100 μ M CALPST-ala having no influence $(p<6\times10^{-5})$. Thus, the 100 μ M CALPST inhibitory CCI effects at both 48 and 96 h are significantly different from CCI for corresponding untreated and CALPST-ala treated controls, and also from CCI for 25 μ M CALPST at both treatment durations (p<0.01 and p<0.0005, respectively). Finally, we found that the inactive inhibitor CALPST-ala has no significant effect on CCI under any conditions tested (Fig. 2). In summary, these results show that the cell-penetrating and calpainspecific inhibitor, CALPST, exhibits dose- and time-dependent inhibitory effects on pericyte contractility.

We next turned to studies aimed at revealing the calpaindependence of talin-enhanced contractility. To this end, pericytes electroporated with pEGFP-talin, or pEGFP-talin L432G were left untreated or treated with CALPST as described (see Materials and methods). As shown in Fig. 1B, when pericytes overexpressing EGFPtalin are treated with 25 µM CALPST for 24 h, there is a 36% reduction in talin-induced contractility $(0.64 \pm 0.1, p < 2 \times 10^{-6})$, as compared to untreated control cells. However, Fig. 3 shows that CALPST treatment does not alter pericyte CCI when cells are transfected with either control pEGFP vector (0.97 \pm 0.12, p = 0.85) or pEGFP-talin L432G $(0.91 \pm 0.09, p = 0.82)$. Thus, the CALPST-dependent reversal of calpain-regulated contractility (in terms of CCI) corroborates data derived from our overexpression studies that indicated pericyte contractility to be talin- and calpain-dependent (Fig. 1). Collectively, these findings reflect the important role that calpain plays in shaping talin-dependent contractility.

Considering that activated RhoA Q63L enhances pericyte contractile force production (Fig. 1) and that RhoA has itself been reported to be a calpain substrate linked to cytoskeletal remodeling (Kulkarni et al., 2002), we then asked to what extent pericyte contractile force

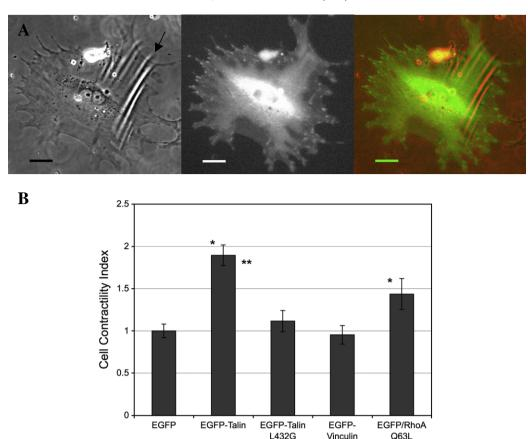


Fig. 1. Molecular control of pericyte contractility. Bovine retinal pericytes were electroporated either with plasmids encoding control EGFP and fusion of EGFP-talin, EGFP-talin L432G (calpain-resistant mutant) or EGFP-vinculin, or co-transfected (in 1:4 ratio) with plasmids encoding EGFP and RhoA Q63L (dominant active mutant). On next day, transfected pericytes were seeded onto deformable silicone substrata. After 24 h live GFP-positive cells were evaluated by microscopy. (A) A pericyte overexpressing EGFP-talin is shown wrinkling silicone substratum (left panel — phase contrast image, central panel — fluorescence image, right panel — overlay image of phase contrast and fluorescence pseudocolored red and green, respectively). An arrow points at cell contraction-driven deformations of the substrata. (B) A graph showing contractile force transduction, as measured by cell contractility index (CCI) and described in Materials and methods, in pericytes overexpressing designated proteins, CCI for EGFP control was equaled to 1, to which other CCI values were normalized. Asterisk (*) indicates statistically significant difference between control EGFP and EGFP-talin (p < 4E - 9), and EGFP/RhoA Q63L (p < 0.04), respectively. Double asterisk (**) indicates statistically significant difference between EGFP-talin and EGFP-talin L432G (p < 2E - 05). The CCI of EGFP-talin L432G and EGFP-vinculin were not statistically significantly different from control EGFP. Scale bar = 30 µm.

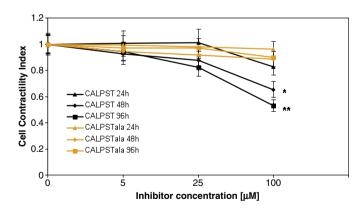


Fig. 2. Calpain regulates pericyte contractile force production. Untransfected pericyte force production, as measured by cell contractility index (CCI, see Materials and methods) was monitored and quantified as a function of calpain inhibition. CALPST and its inactive mutant CALPST-ala were added at final concentrations of 0, 5, 25, and 100 μM for 24, 48 and 96 h of treatment. The inhibitors were added at the time of seeding pericytes onto deformable substrata and re-applied in a fresh medium at 24 h in cultures scored at 48 h, and at 24 and 72 h in cultures scored at 96 h. Asterisk (*) indicates statistically significant differences between pericytes treated with 100 μM CALPST for 48 h and either untreated (p<0.01), treated with 100 μM CALPST-ala for 48 h (p<0.01) or 25 μM CALPST for 48 h (p<0.01). Double asterisk (**) indicates statistically significant differences between pericytes treated with 100 μM CALPST for 96 h and either untreated (p<2.E=0.7), treated with 100 μM CALPST-ala for 96 h (p<6.E=0.5), 100 μM CALPST-ala for 96 h (p<5.E=0.4).

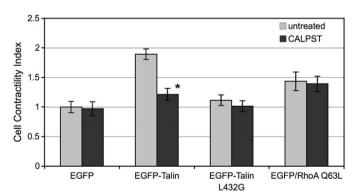


Fig. 3. Talin, but not RhoA-induced pericyte contractility is calpain-dependent. Bovine retinal pericytes were electroporated either with plasmids encoding control EGFP and fusion of EGFP-talin, EGFP-talin L432G (calpain-resistant mutant, or co-transfected (in 1:4 ratio) with plasmids encoding EGFP and RhoA Q63L (dominant active mutant). On the next day, transfected pericytes were seeded onto deformable silicone substrata. After 24 h live GFP-positive cells were evaluated by microscopy. On next day, transfected pericytes were seeded onto deformable silicone substrata, and either left untreated or treated with calpain inhibitor CALPST at 25 μ M final concentration for 24 h. Contractility of samples was analyzed for cell contractility index (CCI) and normalized to untreated EGFP control equaled to 1. Asterisk (*) indicates statistically significant difference between CALPST-treated EGFP-talin and untreated EGFP-talin (p < 2E - 6). CALPST treatment of other cultures does not cause statistically significant differences, as compared with their corresponding untreated controls.

transduction induced by RhoA Q63L would be calpain-dependent. To address this question, we tested whether RhoA Q63L-induced contractility would be modulated when calpain activity is inhibited by CALPST. To this end, pericytes were co-electroporated with a transfection marker, pEGFP, and either pExv–RhoA Q63L or pExv control plasmid. Importantly, while RhoA Q63L increases contractility (1.44 \pm 0.18, p<0.05; Fig. 1B), pericyte CCI remains unaffected when RhoA L63-overexpressing cells are treated with CALPST (1 vs. 0.97 \pm 0.13, p=0.52; Fig. 3). These results demonstrate that, unlike talin-enhanced contractility, RhoA-induced contractility is not calpain-sensitive.

Calpain controls contractile related stiffness measured by AFM nanoindentation

AFM-enabled nanoindentation allows for direct physical measurement of local elastic properties of living pericytes (Lee et al., 2010), and thus enables correlations between cell contraction-induced silicone wrinkling and local cellular stiffness parameters (Fig. 4B). We measured effective elastic moduli ($E_{\rm eff}$) of subcellular regions located just above wrinkled domains of the deformable silicone substrata, corresponding to stress fiber-enriched subcellular domains, (Fig. 4A) as well as subcellular regions that are devoid of stress fibers, which are located above substrata that are not actively being deformed (i.e., divorced from wrinkled substratum regions, Fig. 4C). Although these $E_{\rm eff}$ are not intended to represent the mechanical

stiffness of the entire cell, such experiments provide quantitative comparisons of the mechanical differences in contractile vs. noncontractile regions of the pericyte. These measurements evaluated regions of untreated cells, as well as cells treated with 100 µM CALPST or its inactive mutant CALPST-ala for 24 h. In untreated cells, $E_{\rm eff}$ measured on unwrinkled domains is lower (0.8 \pm 0.05, p<0.05) as compared to wrinkled domains, thus correlating increased local cell stiffness with enhanced contractile strain. We have shown previously that, as expected, these regions of increased subcellular stiffness at wrinkled substrata are also regions of actin cytoskeletal bundles (Lee et al., 2010). Interestingly, inhibition of calpain by CALPST causes a statistically significant increase in stiffness on wrinkled domains (1.3 \pm 0.07, p<0.001 or 1.31 \pm 0.07, p<0.001), as compared to such regions in untreated cells or in CALPST-ala treated cells, respectively (Fig. 4D). Thus, the difference in $E_{\rm eff}$ between wrinkled and unwrinkled domains in CALPST-treated cells is markedly enhanced (p < 0.001) when compared to untreated cells (p < 0.05). This effect of CALPST on subcellular stiffness is calpain-specific. since this effect is not observed in CALPST-ala treated cells. In addition, $E_{\rm eff}$ on unwrinkled domains is essentially unchanged in either CALSPT or CALPST-ala treated cells, as compared to untreated controls (p = 0.825, Fig. 4D). This result indicates that inhibition of calpain activity leads to locally increased stiffness during cell contraction, whereas elastic properties of non-contractile regions remain unchanged.

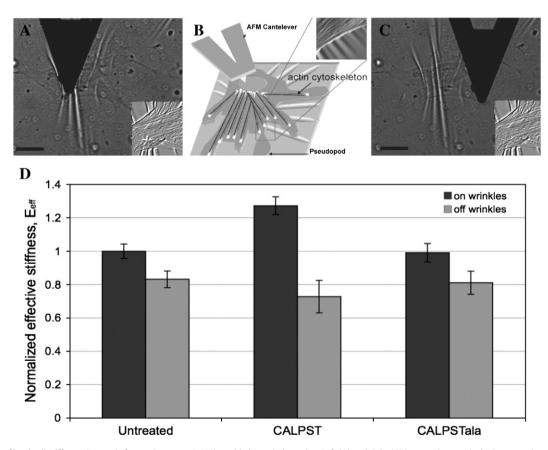


Fig. 4. Assessment of local cell stiffness via atomic force microscope (AFM)-enabled nanoindentation. Left (A) and right (C) images show optical microscopy images of the cantilever positioned directly above and far from wrinkled regions of the silicone substrata, respectively (on-wrinkle and off-wrinkle, respectively). Black arrowheads indicate wrinkles observable in silicone substrate. Central diagram (B) demonstrates the experimental setup, wherein pericytes were grown on deformable silicone substrata and exhibited actin stress fibers (also marked by the star in left inset); pericyte contractile forces deformed or wrinkled the substratum, and indentation of subcellular regions was conducted near and far from regions of visible substrata contraction. Insets in (A)–(C) show AFM deflection images of pericytes and underlying silocone substrata with cell-generated wrinkle deformations. (D) Subcellular stiffness expressed as indentation effective elastic moduli $E_{\rm eff}$ at on- and off-wrinkle positions, as a function of exposure to calpain inhibitor CALPST (100 μM final concentration, 24 h). At least five cells were analyzed per condition, and data are normalized by the value of $E_{\rm eff}$ for the untreated cells on-wrinkle stiffness. Asterisk (*) indicates statistically significant difference in $E_{\rm eff}$ between on-wrinkle locations (p<0.05); and plus sign (‡) indicates statistically significant difference in $E_{\rm eff}$ between CALPST-treated on-wrinkle and off-wrinkle (p<0.001). Scale bar = 20 μm.

Discussion

In this study, we demonstrate that calpain and talin play pivotal roles in modulating multiple aspects of pericyte-generated strains and contractile force transduction. In particular, we show that talin, but not its calpain-resistant mutant or its binding partner vinculin, contributes markedly to the extent of pericyte contractility. These results, together with our earlier described calpain cleavage studies of endogenous talin (Croce et al., 1999) and of EGFP-talin (Franco et al., 2004), point to the importance of calpain-mediated talin cleavage as a mechanism for regulating cellular contractility. We also demonstrate that calpain control of talin-enhanced contractility apparently operates upstream or in parallel to RhoA-regulated cytoskeletal remodeling since calpain inhibition can reverse talin-induced but, not RhoA L63-regulated pericyte contraction. Moreover, calpain's control over pericyte contractility is apparent whether using cell-penetrating calpain-specific inhibitors in single cell-based contractility assays or using direct measurement of subcellular stiffness via AFM-enabled nanoindentation. These findings significantly extend earlier studies aimed at understanding the Rho GTPand cytoskeletal-dependent mechanisms that control pericyte contractility (Herman and D'Amore, 1985; Kolyada et al., 2003; Kutcher et al., 2007; Kutcher and Herman, 2009; Lee et al., 2010).

Calpain and talin control pericyte contractility

Using CCI, we observed that EGFP-talin overexpression significantly enhances pericyte contractility as compared to control cells overexpressing EGFP alone (Fig. 1). These observations are consistent with the studies in which talin 1 has been shown to be necessary for reinforcement of integrin-mediated adhesion, linkage to actin cytoskeleton, and support of mechanotransduction in murine fibroblasts (Roca-Cusachs et al., 2009; Zhang et al., 2008). On the contrary, we observed no change of contractility in pericytes overexpressing a point mutant of talin, L432G (Fig. 1B). Indeed, endogenous talin and EGFP-talin have been demonstrated to be cleaved by calpain (Croce et al., 1999 and Franco et al., 2004, respectively), whereas EGFP-talin L432G mutant has been shown to be resistant to calpain cleavage and to inhibit focal adhesion dynamics (Franco et al., 2004), Importantly, we observe differential effects of wild-type and mutant talin L432G overexpression on pericyte contractility. This cannot be attributed to differential localization of talin and this mutant in focal adhesions, as previous studies have confirmed comparable patterns of FA-specific localization for both wild-type and mutant talin L432G (Franco et al., 2004). Additionally, talin and its L432G mutant exhibit comparable ability to interact with FAK and focal adhesion-targeted type I phospatidylinositol phosphate kinase (PIPKy66) as well as to activate integrin (Franco et al., 2004). In this context, our results are consistent with the calpain-dependent cleavage of talin as a critical step in controlling pericyte contractility, perhaps via modulating FA dynamics. This hypothesis is supported by the observable time- and dosedependent CCI inhibitory effect of CALPST, but not of its mutant CALPST-ala (Fig. 2). Observations of the time-dependent CALSPT inhibition on pericyte contractility (Fig. 2) can be related to previous reports describing calpain as an abundant and long-lived enzyme with half-life of approximately five days (Zhang et al., 1996). This may explain why low concentrations and early timepoints for CALPST treatment regimens (e.g., 25 µM at 24 hr) are seemingly below an observable threshold for inhibiting spontaneous pericyte contractility. Taken together, these data indicate that talin- and calpain-mediated signaling modulates pericyte contractility.

Talin, but not vinculin, enhances pericyte contractility in calpain-dependent fashion

Having established a critical role for calpain-dependent talin cleavage during cell contraction, we sought to determine whether vinculin would also play a role in contractile force transduction. By comparing effects of overexpressed talin to overexpressed vinculin in the deformable silicone substrata assay, we showed that vinculin overexpression does not alter pericyte contractility (Fig. 1B), whereas talin overexpression does increase contractility. This finding is consistent with the report that calpain cleavage of talin is a ratelimiting step in controlling vinculin disassembly from FAs (Franco et al., 2004). In addition, despite the well-documented presence of vinculin in all integrin-containing FA structures (Gilmore and Burridge, 1996; Craig and Chen, 2003; Zimerman et al., 2004; Chen et al., 2005), it is widely reported that organization of FAs at the membrane critically depends on integrin-talin binding but not on vinculin (Moulder et al., 1996; Xu et al., 1998). Talin has also been demonstrated to be the most strongly bound component in the FA protein network (Lele et al., 2008). Furthermore, although vinculin has been suggested to contribute to strength of cell adhesion (Gallant et al., 2005) and to act as a target for calpain cleavage (Goll et al., 2003; Weber et al., 2009), it has also been shown that mechanical stretching of talin unmasks its vinculin binding sites (del Rio et al., 2009). Thus, it is likely that vinculin recruitment and activation in FAs (Chen et al., 2006) depends strongly on presence and conformation of talin. Indeed, the present results demonstrate the central role that talin, but not vinculin, possesses in modulating pericyte contractility.

Calpain alters contractility by differential control of talin, but not of activated RhoA

The RhoA/Rho kinase pathway is critically involved in many aspects of cardiovascular physiology and pathophysiology (Loirand et al., 2006; Pacaud et al., 2005). Furthermore, since RhoA has been reported to be a calpain substrate (Goll et al., 2003), it was important to consider possible roles of calpain in RhoA-induced effects on pericyte contractility. Our previous work demonstrated that Rho GTP-dependent induction of pericyte contraction occurs in a α SMAspecific, but not non-muscle isoactin-dependent manner (Kolyada et al., 2003; Kutcher et al., 2007). These earlier findings are consistent with our observations indicating that constitutively active RhoA Q63L enhances contractility. Importantly, however, we now appreciate that RhoA-driven pericyte contractility is not calpaindependent, since contractility is not reversible by the calpainspecific inhibitor CALPST (Fig. 3). Together, these data point to the possibility that active RhoA and calpain signal through the cytoskeletal network to influence contractile force transduction via parallel pathways. Indeed, the same constitutively active mutant of RhoA Q63L enhances bovine aortic endothelial (BAE) cell spreading, FA assembly and stress fiber formation even in the presence of the calpain inhibitor, calpeptin (Kulkarni et al., 1999). Similarly, calpaindependent remodeling of FA components may influence adhesiondependent and contractile mechanisms in an isoactin-dependent manner. For example, endothelial cells express non-muscle (β, γ) isoactins while pericytes express non-muscle (β, γ) and smooth muscle (α) contractile protein isoforms (Kutcher and Herman, 2009; Herman and D'Amore, 1985). That pericyte and endothelial RhoA signaling is seemingly calpain-insensitive suggests that earlier, upstream events modulate the calpain-, Rac- and RhoA-dependent signaling events that contribute to altered cell shape and contractile phenotype observed by us and by others (Bialkowska et al., 2000). This may also explain why we could not observe any increase in Rhoinduced pericyte contractility in cells treated with CALPST; and that CALPST treatment did not reduce active RhoA-induced contractility, but could completely reverse talin-enhanced contractility as quantified by CCI (Fig. 3). These data are consistent with a model which postulates that calpain operates upstream of active RhoA, enabling talin cleavage to differentially control contractile force transduction at mature focal adhesions.

Calpain modulates stiffness of pericyte contractile domains

Local effective stiffness of subcellular domains $E_{\rm eff}$ was quantified in contractile pericytes via AFM-enabled indentation, both at cell locations just above the substrata wrinkles ("wrinkled domains") and at cell locations remote from those contractile zones ("unwrinkled domains"). We found that $E_{\rm eff}$ of the stress fiber-enriched pericyte domains at substrata wrinkles was greater than the subcellular stiffness far from such wrinkles (Fig. 4), as is consistent with the stress fiber enrichment at the "wrinkled domains". Importantly, $E_{\rm eff}$ markedly increased in response to calpain inhibition by CALPST (Fig. 4). CALPST also decreased the number of contractile substrata deformations per cell as quantified by CCI (Fig. 2), viz. local cell stiffness at sites of substrata wrinkling was increased, but the ability of cells to deform their underlying substrata was decreased in response to calpain inhibition.

The observed increase in stiffness of the subcellular contractile regions in response to calpain inhibition can be explained readily by the regulatory role(s) that calpain-mediated remodeling of focal adhesionassociated cytoskeletal proteins play in modifying these extracellular matrix-interacting, cytoskeletal-plasma membrane contact zones. As has been shown by our laboratory (Potter et al., 1998) and others (Franco et al., 2004), calpain-dependent remodeling of the actinassociated cytoskeleton is needed for protrusion formation and cell spreading as well as remodeling the focal contact-enriched membrane anchoring domains needed to disengage rearward adhesions such that cellular translocation can be fostering (by transiently disengaging focal adhesions via calpain-mediated talin proteolysis (Franco et al., 2004). Results of our studies not only support these earlier findings, but demonstrate that inhibition of calpain-dependent cytoskeletal (talin) remodeling gives rise to enhanced stability of existing adhesion complexes, a greater persistence of the actin-rich stress fibers and a locally elevated mechanical stiffness linked to decreased talin and focal adhesion turnover. Further, we reason that there are likely to be indirect effects of calpain inhibition on cytoskeletal effectors, which might include a potential increase in RhoA activation through effects on the guanine exchange or activating proteins (GEF/GAP), as has been suggested by others (Kulkarni et al., 2002; Mammoto et al., 2007; Miyazaki et al., 2010). Such increased RhoA activation would induce higher contractile force production outside of the calpain-regulated cytoskeletal effector pathways involved in regulating cell shape and motility since CALPST treatment of living pericytes has no effect on RhoA-regulated cytoskeletal remodeling (Fig. 3). On the other hand, there is one report suggesting opposing effects of calpain on RhoAdependent cytoskeletal remodeling (Gonscherowski et al., 2006). This contrast may be cell- or contractile protein isoform-specific since the RhoA- and calpain-dependent mechanisms that control contractility and/or force transduction in non-muscle or smooth muscle-like cells may not be identical (Herman and D'Amore, 1985; Kolyada et al., 2003; Kutcher and Herman, 2009; Kutcher et al., 2007; Durham and Herman,

Given the dynamic nature pericyte-driven deformation of elastic substrata, the observations that CALPST treatment of living cells yields differential effects on cytoskeletal-dependent contractile events, i.e. decreased CCI and increased $E_{\rm eff}$, suggests that calpain regulates a dynamic interplay involved in generating or sustaining those cellular forces needed for isotonically- and/or isometrically-contracting cytoplasmic domains. For example, we seldom observe deformed substrata underlying regions of advancing cytoplasm actively engaged in isotonically contracting F-actin-rich cytoplasmic domains (distal reaches of pseudopods, filapods and membrane ruffles). This is in stark contradistinction to the actively deformed zones of elastic substrata beneath domains that we posit to be engaged in isometric contraction where force transduction is occurring in the absence of stress fiber length or cell shape changes. We reason that such a calpain-controlled balance in pericyte contractility likely depends on the

dynamics of FA assembly/turnover, which has been shown to calpainand talin-dependent (Franco et al., 2004). Moreover, our results also suggest a controlling role for calpain in a positive feedback loop existing between force transduction and FA stabilization (Balaban et al., 2001; Bershadsky et al., 2006; Burridge and Chrzanowska-Wodnicka, 1996). Indeed, this dynamically reciprocal signaling loop could likely be controlled by calpain, which cleaves talin and fosters β integrin subunit dissociation from other FA- and cytoskeletal-associating proteins (Franco and Huttenlocher, 2005). However, such control could be lost with calpain inhibition, resulting in (i) non-cleaved talin, (ii) inhibition of FA turnover and (iii) enhanced local stiffening. This hypothesis is consistent with our observations of decreased CCI and increased $E_{\rm eff}$ above or "on" substrata wrinkles in response to calpain inhibitor CALPST. In addition, the observation of increased stiffness (E_{eff} at substrata-wrinkled domains) is consistent with the reported enlargement of paxillin- and vinculin-containing FAs caused by talin L432G expressed in talin 1 null cells (Franco et al., 2004), which could likely lead to FA stabilization, increased association of filamentous actin, and thus be coupled with increased magnitude of contractile force. Our combined data suggest a preliminary model wherein increases in Rho GTP-dependent cytoskeletal contractile events anchored at the FA are countered via calpain-dependent modulation of cellular mechanotransduction. Thus, by selectively targeting key FA-associated cytoskeletal substrates, such as talin, pericytes' control of contractile forces against adherent substrata (extracellular matrix and basement membrane) or adjacent microvascular endothelial cells (cell-cell association) could be regulated. More detailed studies of the kinetics and distribution of contractile forces, as well as of calpain-dependent signaling pathways and mechanisms involved in generation of these forces, are needed to further elucidate and validate such a regulatory model.

Calpain control of cellular contractility and human pathogenesis

In addition to identifying calpain and talin functional interactions as an important regulatory mechanism of cell contractility in general, our results offer insights into phenomena that underlie microvascular disorders such as in retinopathies. The calpain pathway has been implicated in as a mechanism of apoptotic retinal cell death produced by elevated intraocular pressure and hypoxia leading to retinal degenerations associated with glaucoma and retinitis pigmentosa (Paquet-Durand et al., 2007; Azuma and Shearer, 2008). Moreover, deregulated contractility of pericytes has been postulated as a potential, chemomechanically transduced cause of microvascular endothelial hyperproliferation and perturbed tone in pathogenesis of diabetic and age related retinopathies (Kutcher and Herman, 2009; Kutcher et al., 2007). Additionally, deregulated contractile force transduction seems an even more relevant target of investigation and potential therapeutic interventions, as we have most recently demonstrated that the strains exerted by pericytes onto substrata can be sufficient to alter the effective elastic moduli of basement membrane; this substrata stiffening would provide indirect modulation of the EC mechanical microenvironment, in addition to the direct mechanical strain pericytes can exert via contraction (Lee et al., 2010). Further investigation into the effects of FA manipulations on pericytedependent EC growth control would validate this hypothesis of such a mechanism contributing to microvascular disorders.

Acknowledgments

We gratefully acknowledge the US National Science Foundation CAREER Award (KJVV), US National Defense Science and Engineering Graduate Fellowship program (ASZ), Singapore-MIT Alliance in Research & Technology BioSyM, NIH EY 19533 and NIH EY 15125 (IMH). We thank David Potter for longstanding collaborations and scholarly discussions and Jeffry Deckenback for critical reading of the manuscript, including assistance with figure preparation.

References

- Aebi, U., Pollard, T.D., 1987. A glow discharge unit to render electron microscope grids and other surfaces hydrophilic. J. Electron Microsc. Tech. 7, 29–33.
- Arnaout, M.A., Goodman, S.L., Xiong, J.P., 2007. Structure and mechanics of integrinbased cell adhesion. Curr. Opin. Cell Biol. 19, 495-507.
- Azuma, M., Shearer, T.R., 2008. The role of calcium-activated protease calpain in experimental retinal pathology. Surv. Ophthalmol. 53, 150–163.
- Balaban, N.Q., Schwarz, U.S., Riveline, D., Goichberg, P., Tzur, G., Sabanay, I., Mahalu, D., Safran, S., Bershadsky, A., Addadi, L., Geiger, B., 2001. Force and focal adhesion assembly: a close relationship studied using elastic micropatterned substrates. Nat. Cell Biol. 3, 466-472.
- Banno, A., Ginsberg, M.H., 2008. Integrin activation. Biochem. Soc. Trans. 36, 229–234. Benjamin, L.E., Hemo, I., Keshet, E., 1998. A plasticity window for blood vessel remodelling is defined by pericyte coverage of the preformed endothelial network and is regulated by PDGF-B and VEGF. Development 125, 1591–1598.
- Berrier, A.L., Yamada, K.M., 2007. Cell-matrix adhesion. J. Cell. Physiol. 213, 565-573. Bershadsky, A.D., Ballestrem, C., Carramusa, L., Zilberman, Y., Gilquin, B., Khochbin, S., Alexandrova, A.Y., Verkhovsky, A.B., Shemesh, T., Kozlov, M.M., 2006. Assembly and mechanosensory function of focal adhesions: experiments and models. Eur. J. Cell Biol. 85, 165-173.
- Bialkowska, K., Kulkarni, S., Du, X., Goll, D.E., Saido, T.C., Fox, J.E., 2000. Evidence that beta3 integrin-induced Rac activation involves the calpain-dependent formation of integrin clusters that are distinct from the focal complexes and focal adhesions that form as Rac and RhoA become active. J. Cell Biol. 151, 685-696.
- Bjarnegard, M., Enge, M., Norlin, J., Gustafsdottir, S., Fredriksson, S., Abramsson, A., Takemoto, M., Gustafsson, E., Fassler, R., Betsholtz, C., 2004. Endothelium-specific ablation of PDGFB leads to pericyte loss and glomerular, cardiac and placental abnormalities. Development 131, 1847-1857.
- Burridge, K., Chrzanowska-Wodnicka, M., 1996. Focal adhesions, contractility, and signaling. Annu. Rev. Cell Dev. Biol. 12, 463-518.
- Chen, H., Cohen, D.M., Choudhury, D.M., Kioka, N., Craig, S.W., 2005. Spatial distribution and functional significance of activated vinculin in living cells. J. Cell Biol. 169, 459-470.
- Chen, H., Choudhury, D.M., Craig, S.W., 2006. Coincidence of actin filaments and talin is required to activate vinculin. J. Biol. Chem. 281, 40389-40398.
- Cortesio, C.L., Chan, K.T., Perrin, B.J., Burton, N.O., Zhang, S., Zhang, Z.Y., Huttenlocher, A., 2008. Calpain 2 and PTP1B function in a novel pathway with Src to regulate invadopodia dynamics and breast cancer cell invasion. J. Cell Biol. 180, 957-971.
- Craig, S.W., Chen, H., 2003. Lamellipodia protrusion: moving interactions of vinculin and Arp2/3. Curr. Biol. 13, R236-R238.
- Croall, D.E., Ersfeld, K., 2007. The calpains: modular designs and functional diversity. Genome Biol. 8, 218.
- Croce, K., Flaumenhaft, R., Rivers, M., Furie, B., Furie, B.C., Herman, I.M., Potter, D.A., 1999. Inhibition of calpain blocks platelet secretion, aggregation, and spreading. J. Biol. Chem. 274, 36321-36327.
- Darland, D.C., D'Amore, P.A., 1999. Blood vessel maturation: vascular development comes of age. J. Clin. Invest. 103, 157-158.
- Darland, D.C., D'Amore, P.A., 2001a. Cell-cell interactions in vascular development. Curr. Top. Dev. Biol. 52, 107-149.
- Darland, D.C., D'Amore, P.A., 2001b. TGF beta is required for the formation of capillarylike structures in three-dimensional cocultures of 10T1/2 and endothelial cells. Angiogenesis 4, 11-20.
- Darland, D.C., Massingham, L.J., Smith, S.R., Piek, E., Saint-Geniez, M., D'Amore, P.A., 2003. Pericyte production of cell-associated VEGF is differentiation-dependent and is associated with endothelial survival. Dev. Biol. 264, 275-288.
- del Rio, A., Perez-Jimenez, R., Liu, R., Roca-Cusachs, P., Fernandez, J.M., Sheetz, M.P., 2009. Stretching single talin rod molecules activates vinculin binding. Science 323, 638-641. Durham, J.T., Herman, I.M., 2009. Inhibition of angiogenesis in vitro: a central role for
- beta-actin dependent cytoskeletal remodeling. Microvasc. Res. 77, 281-288 Folkman, J., 1971. Tumor angiogenesis: therapeutic implications. N. Engl. J. Med. 285,
- Franco, S.J., Huttenlocher, A., 2005. Regulating cell migration: calpains make the cut. J. Cell Sci. 118, 3829-3838.
- Franco, S.J., Rodgers, M.A., Perrin, B.J., Han, J., Bennin, D.A., Critchley, D.R., Huttenlocher, A., 2004. Calpain-mediated proteolysis of talin regulates adhesion dynamics. Nat. Cell Biol. 6, 977-983.
- Gallant, N.D., Michael, K.E., Garcia, A.J., 2005. Cell adhesion strengthening: contributions of adhesive area, integrin binding, and focal adhesion assembly. Mol. Biol. Cell 16,
- Gilmore, A.P., Burridge, K., 1996. Regulation of vinculin binding to talin and actin by phosphatidyl-inositol-4-5-bisphosphate. Nature 381, 531-535.
- Gingras, A.R., Bate, N., Goult, B.T., Hazelwood, L., Canestrelli, I., Grossmann, J.G., Liu, H., Putz, N.S., Roberts, G.C., Volkmann, N., Hanein, D., Barsukov, I.L., Critchley, D.R., 2008. The structure of the C-terminal actin-binding domain of talin. EMBO J. 27, 458-469.
- Goll, D.E., Thompson, V.F., Li, H., Wei, W., Cong, J., 2003. The calpain system. Physiol. Rev. 83, 731-801.
- Gonscherowski, V., Becker, B.F., Moroder, L., Motrescu, E., Gil-Parrado, S., Gloe, T., Keller, M., Zahler, S., 2006. Calpains: a physiological regulator of the endothelial barrier? Am. J. Physiol. Heart Circ. Physiol. 290, H2035-H2042.
- Hanna, R.A., Campbell, R.L., Davies, P.L., 2008. Calcium-bound structure of calpain and its mechanism of inhibition by calpastatin. Nature 456, 409-412.
- Harris, A.K., Wild, P., Stopak, D., 1980. Silicone rubber substrata: a new wrinkle in the study of cell locomotion. Science 208, 177-179.
- Healy, A.M., Herman, I.M., 1992. Density-dependent accumulation of basic fibroblast growth factor in the subendothelial matrix. Eur. J. Cell Biol. 59, 56-67.

- Herman, I.M., D'Amore, P.A., 1985, Microvascular pericytes contain muscle and nonmuscle actins. J. Cell Biol. 101, 43–52.
- Huttenlocher, A., Palecek, S.P., Lu, Q., Zhang, W., Mellgren, R.L., Lauffenburger, D.A., Ginsberg, M.H., Horwitz, A.F., 1997. Regulation of cell migration by the calciumdependent protease calpain. J. Biol. Chem. 272, 32719–32722.
- Hynes, R.O., 2002. Integrins: bidirectional, allosteric signaling machines. Cell 110, 673-687. Izard, T., Vonrhein, C., 2004. Structural basis for amplifying vinculin activation by talin. J. Biol, Chem. 279, 27667-27678.
- Jain R.K. 2003. Molecular regulation of vessel maturation. Nat. Med. 9, 685–693.
- Kolyada, A.Y., Riley, K.N., Herman, I.M., 2003. Rho GTPase signaling modulates cell shape and contractile phenotype in an isoactin-specific manner. Am. J. Physiol. Cell Physiol 285 C1116-C1121
- Kulkarni, S., Saido, T.C., Suzuki, K., Fox, J.E., 1999. Calpain mediates integrin-induced signaling at a point upstream of Rho family members. J. Biol. Chem. 274, 21265-21275.
- Kulkarni, S., Goll, D.E., Fox, J.E., 2002. Calpain cleaves RhoA generating a dominantnegative form that inhibits integrin-induced actin filament assembly and cell spreading. J. Biol. Chem. 277, 24435-24441.
- Kutcher, M.E., Herman, I.M., 2009. The pericyte: cellular regulator of microvascular blood flow. Microvasc. Res. 77, 235-246.
- Kutcher, M.E., Kolyada, A.Y., Surks, H.K., Herman, I.M., 2007. Pericyte Rho GTPase mediates both pericyte contractile phenotype and capillary endothelial growth state, Am. I. Pathol, 171, 693-701.
- Lee, S., Zeiger, A., Maloney, J., Kotecki, M., Van Vliet, K.J., Herman, I.M., 2010. Pericyte actomyosin-mediated contraction at the cell-material interface can modulate the microvascular niche. J. Phys. Condens. Matter 22.
- Lele, T.P., Thodeti, C.K., Pendse, J., Ingber, D.E., 2008. Investigating complexity of proteinprotein interactions in focal adhesions. Biochem. Biophys. Res. Commun. 369, 929-934.
- Loirand, G., Guerin, P., Pacaud, P., 2006. Rho kinases in cardiovascular physiology and pathophysiology. Circ. Res. 98, 322-334.
- Ma, H., Tochigi, A., Shearer, T.R., Azuma, M., 2009. Calpain inhibitor SNJ-1945 attenuates events prior to angiogenesis in cultured human retinal endothelial cells. J. Ocul. Pharmacol. Ther. 25, 409-414.
- Mammoto, A., Huang, S., Ingber, D.E., 2007. Filamin links cell shape and cytoskeletal structure to Rho regulation by controlling accumulation of p190RhoGAP in lipid rafts. J. Cell Sci. 120, 456-467.
- Miyazaki, T., Honda, K., Ohata, H., 2010. m-Calpain antagonizes RhoA overactivation and endothelial barrier dysfunction under disturbed shear conditions. Cardiovasc. Res. 85,
- Moes, M., Rodius, S., Coleman, S.J., Monkley, S.J., Goormaghtigh, E., Tremuth, L., Kox, C., van der Holst, P.P., Critchley, D.R., Kieffer, N., 2007. The integrin binding site 2 (IBS2) in the talin rod domain is essential for linking integrin beta subunits to the cytoskeleton. J. Biol. Chem. 282, 17280-17288.
- Moulder, G.L., Huang, M.M., Waterston, R.H., Barstead, R.J., 1996. Talin requires betaintegrin, but not vinculin, for its assembly into focal adhesion-like structures in the nematode Caenorhabditis elegans. Mol. Biol. Cell 7, 1181-1193
- Orlidge, A., D'Amore, P.A., 1987. Inhibition of capillary endothelial cell growth by pericytes and smooth muscle cells. J. Cell Biol. 105, 1455-1462.
- Pacaud, P., Sauzeau, V., Loirand, G., 2005. Rho proteins and vascular diseases. Arch. Mal. Coeur Vaiss. 98, 249-254.
- Papetti, M., Shujath, J., Riley, K.N., Herman, I.M., 2003. FGF-2 antagonizes the TGF-beta1mediated induction of pericyte alpha-smooth muscle actin expression: a role for myf-5 and Smad-mediated signaling pathways. Invest. Ophthalmol. Vis. Sci. 44, 4994–5005.
- Paquet-Durand, F., Johnson, L., Ekstrom, P., 2007. Calpain activity in retinal degeneration. J. Neurosci. Res. 85, 693-702.
- Potter, D.A., Tirnauer, J.S., Janssen, R., Croall, D.E., Hughes, C.N., Fiacco, K.A., Mier, J.W., Maki, M., Herman, I.M., 1998. Calpain regulates actin remodeling during cell spreading. J. Cell Biol. 141, 647-662.
- Potter, D.A., Srirangam, A., Fiacco, K.A., Brocks, D., Hawes, J., Herndon, C., Maki, M., Acheson, D., Herman, I.M., 2003. Calpain regulates enterocyte brush border actin assembly and pathogenic Escherichia coli-mediated effacement. J. Biol. Chem. 278, 30403-30412.
- Roberts, G.C., Critchley, D.R., 2009. Structural and biophysical properties of the integrinassociated cytoskeletal protein talin. Biophys. Rev. 1, 61-69.
- Roca-Cusachs, P., Gauthier, N.C., Del Rio, A., Sheetz, M.P., 2009. Clustering of alpha(5) beta(1) integrins determines adhesion strength whereas alpha(v)beta(3) and talin enable mechanotransduction. Proc. Natl. Acad. Sci. U. S. A. 106, 16245-16250.
- Rucker, M., Strobel, O., Vollmar, B., Roesken, F., Menger, M.D., 2000. Vasomotion in critically perfused muscle protects adjacent tissues from capillary perfusion failure. Am. J. Physiol. Heart Circ. Physiol. 279, H550-H558.
- Sato, Y., Rifkin, D.B., 1989. Inhibition of endothelial cell movement by pericytes and smooth muscle cells: activation of a latent transforming growth factor-beta 1-like molecule by plasmin during co-culture. J. Cell Biol. 109, 309-315.
- Shih, S.C., Ju, M., Liu, N., Mo, J.R., Ney, J.J., Smith, L.E., 2003. Transforming growth factor beta1 induction of vascular endothelial growth factor receptor 1: mechanism of pericyte-induced vascular survival in vivo. Proc. Natl. Acad. Sci. U. S. A. 100, 15859-15864.
- Shuster, C.B., Herman, I.M., 1995. Indirect association of ezrin with F-actin: isoform specificity and calcium sensitivity. J. Cell Biol. 128, 837–848.
 Sieczkiewicz, G.J., Herman, I.M., 2003. TGF-beta 1 signaling controls retinal pericyte
- contractile protein expression. Microvasc. Res. 66, 190-196.
- Thompson, M.T., Berg, M.C., Tobias, I.S., Rubner, M.F., Van Vliet, K.J., 2005. Tuning compliance of nanoscale polyelectrolyte multilayers to modulate cell adhesion. Biomaterials 26, 6836-6845.
- Thompson, M.T., Berg, M.C., Lichter, J., Tobias, I.S., Rubner, M.F., Van Vliet, K.J., 2006. Biochemical functionalization of polyelectrolyte multilayers can alter mechanical compliance. Biomacromolecules 7, 1990-1995.

- von Tell, D., Armulik, A., Betsholtz, C., 2006. Pericytes and vascular stability. Exp. Cell Res. 312, 623–629.
- Weber, H., Huhns, S., Luthen, F., Jonas, L., 2009. Calpain-mediated breakdown of cytoskeletal proteins contributes to cholecystokinin-induced damage of rat pancreatic acini. Int. J. Exp. Pathol. 90, 387–399.
- Wegener, K.L., Partridge, A.W., Han, J., Pickford, A.R., Liddington, R.C., Ginsberg, M.H., Campbell, I.D., 2007. Structural basis of integrin activation by talin. Cell 128, 171–182.
- Wilkinson-Berka, J.L., Babic, S., De Gooyer, T., Stitt, A.W., Jaworski, K., Ong, L.G., Kelly, D. J., Gilbert, R.E., 2004. Inhibition of platelet-derived growth factor promotes pericyte loss and angiogenesis in ischemic retinopathy. Am. J. Pathol. 164, 1263–1273.
- loss and angiogenesis in ischemic retinopathy. Am. J. Pathol. 164, 1263–1273. Xu, W., Baribault, H., Adamson, E.D., 1998. Vinculin knockout results in heart and brain defects during embryonic development. Development 125, 327–337.
- Zaidel-Bar, R., Itzkovitz, S., Ma'ayan, A., Iyengar, R., Geiger, B., 2007. Functional atlas of the integrin adhesome. Nat. Cell Biol. 9, 858–867.
- Zamir, E., Geiger, B., 2001. Molecular complexity and dynamics of cell-matrix adhesions. J. Cell Sci. 114, 3583–3590.
- Zhang, W., Lane, R.D., Mellgren, R.L., 1996. The major calpain isozymes are long-lived proteins. Design of an antisense strategy for calpain depletion in cultured cells. J. Biol. Chem. 271, 18825–18830.
- Zhang, X., Jiang, G., Cai, Y., Monkley, S.J., Critchley, D.R., Sheetz, M.P., 2008. Talin depletion reveals independence of initial cell spreading from integrin activation and traction. Nat. Cell Biol. 10, 1062–1068.
- Zimerman, B., Volberg, T., Geiger, B., 2004. Early molecular events in the assembly of the focal adhesion–stress fiber complex during fibroblast spreading. Cell Motil. Cytoskeleton 58, 143–159.